

Analysis of Gas Disturbance Characteristics in Lunar Sample Storage

Lv Shizeng, Han Xiao, Zhang Yi, Ding Wenjing

Abstract—The lunar sample storage device is mainly used for the preparation of the lunar samples, observation, physical analysis and other work. The lunar samples and operating equipment are placed directly inside the storage device. The inside of the storage device is a high purity nitrogen environment to ensure that the sample is not contaminated by the Earth's environment. In order to ensure that the water and oxygen indicators in the storage device meet the sample requirements, a dynamic gas cycle is required between the storage device and the external purification equipment. However, the internal gas disturbance in the storage device can affect the operation of the sample. In this paper, the storage device model is established, and the tetrahedral mesh is established by Tetra/Mixed method. The influence of different inlet position and gas flow on the internal flow field disturbance is calculated, and the disturbed flow area should be avoided during the sampling operation.

Keywords—Lunar samples, gas disturbance, storage device, characteristic analysis.

I. INTRODUCTION

HUMANS have landed on the moon, and brought back some of the lunar soil and rock samples.

Between 1969 and 1972, the United States brought 382 kilograms of lunar samples from the lunar surface through six Apollo space missions. In addition, the former Soviet Union's three automated spacecraft also brought back important samples from three different locations of the moon, a total of 300 grams [1]. Before the samples were collected on the moon, they had millions to billions of years in a vacuum. If these samples are exposed to damp air in the earth, they will react chemically. The iron elements in the sample react with the oxygen in the air to form rust, and the minerals in the sample react with the water in the air to form clay.

The Lunar sample storage device is mainly used for the preparation of samples, observation, physical property analysis and so on. The interior of the storage device is a high purity nitrogen environment. The use of high purity nitrogen in the device will effectively prevent the sample from reacting with the surrounding environment and maintain the purity of the Lunar sample.

To ensure the purity of nitrogen in the device to meet the

Lv Shizeng is with the Beijing Institute of Spacecraft Environment Engineering, China Academy of Space Technology, Beijing, CO 10094 China (phone: +86-10-68747259-614; fax: +86-10-68746751; e-mail: Lvshizeng@163.com).

Han Xiao is with the School of Astronautics, Beihang University, Beijing, China, working in Beijing Institute of Spacecraft Environment Engineering, China Academy of Space Technology, Beijing, CO 10094 China.

Zhang Yi and Ding Wenjing are with the Beijing Institute of Spacecraft Environment Engineering, China Academy of Space Technology, Beijing, CO 10094 China.

storage requirements of the Lunar sample, a closed cycle was required between the device and the external purification equipment to maintain purity of the nitrogen within a required range. The gas circulation process between the purification equipment and the storage device is shown in Fig. 1.

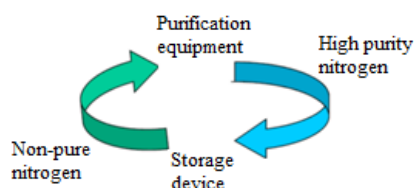


Fig. 1 The gas circulation process between the purification equipment and the storage device

In this paper, the gas disturbance in the storage device was simulated to confirm the gas inlet and outlet position and its internal disturbance distribution, so as to provide reference for the operation of the sample.

II. PHYSICAL MODEL

The storage device is shown in Fig. 2. The main storage area is the box structure; the front and rear panels are transparent glass. The internal size of the main storage area is 1250 mm x 780 mm x 900 mm; the size of the bracket is 796 mm x 280 mm, thickness is 2 mm. The bracket is divided into two layers, and the distance from the bottom plate is 300 mm and 500 mm respectively.

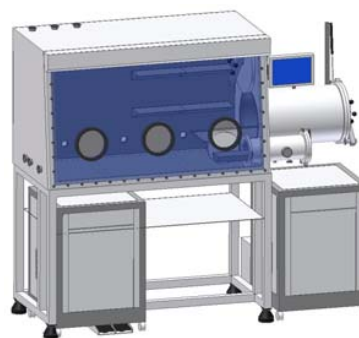


Fig. 2 Lunar sample storage device model

III. CALCULATION OF THE INFLUENCE OF DIFFERENT INLET POSITIONS ON THE MAIN OPERATING AREA

A. Structure of Top-Entering and Bottom-Out

The gas inside the tank flows into the main storage area from

the top and flows out of main storage area at the bottom.

In order to better describe the air flow in the tray area, a total of four cross sections are selected in Fig. 3, i.e., $Y = 0.25$ m, $X = 0$ m, 0.25 m and 0.45 m. The tetrahedral mesh was established by Tetra/Mixed method [2], [3]. In the simulation circulation, the turbulence model is selected as k-epsilon [4], [5] and the parameters of the nitrogen are invoked from the material library of the simulation software. The inlet is then set as the Velocity Inlet, and the exit is set to Outflow Boundary.

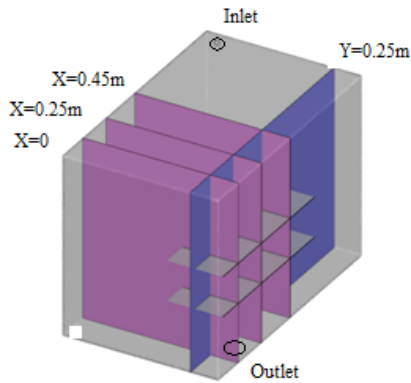


Fig. 3 Calculation model of top-entering and bottom-out structure

Fig. 4 shows the velocity vector of $Y = 0.25$ m cross section at 0.8 m/s wind velocity. Fig. 5 shows the $Y = 0.25$ m cross section velocity sketch at $V = 0.8$ m/s. It can be seen from Figs. 4 and 5 that when the blowing speed is 0.8 m/s, there are eddy

currents in the area above the two-stage brackets, and the flow intensity of the large area near the upper side of the second layer is obviously larger than that of other regions, as well as stronger in sweeping the air.

The main operation area on the left side of the box airflow disturbance is not conducive to the operation of the sample.

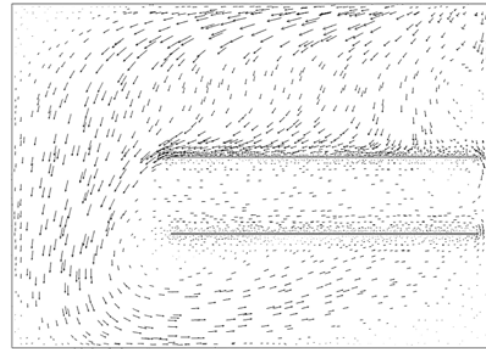


Fig. 4 $V = 0.8$ m/s, $Y = 0.25$ m cross section velocity vector

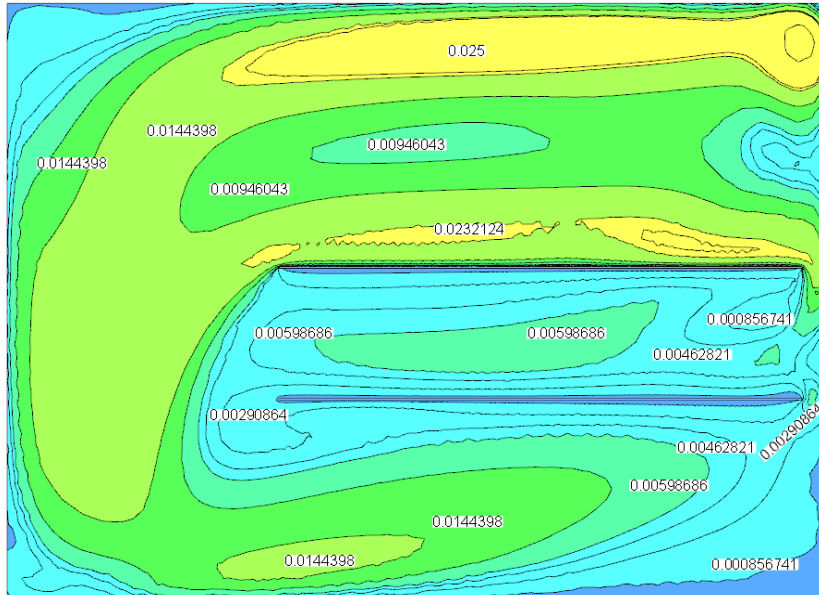
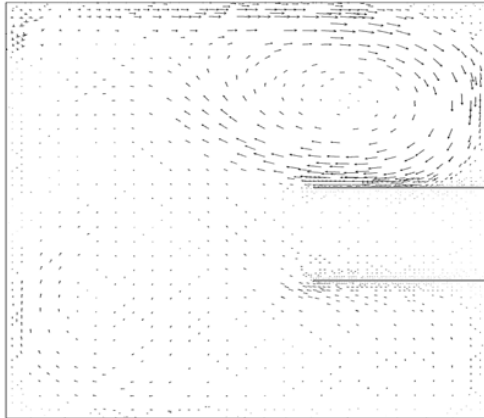


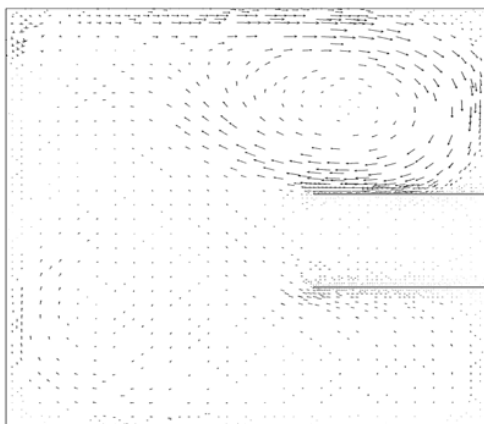
Fig. 5 $V = 0.8$ m/s, $Y = 0.25$ m cross section velocity sketch

Fig. 6 shows the velocity vector of $X = 0$ m, 0.25 m and 0.45 m cross sections at 0.8 m/s wind speed. As can be seen from Fig. 6, the flow intensity of the first layer of the brackets is weak, and the vortex is mainly presented on the upper side of

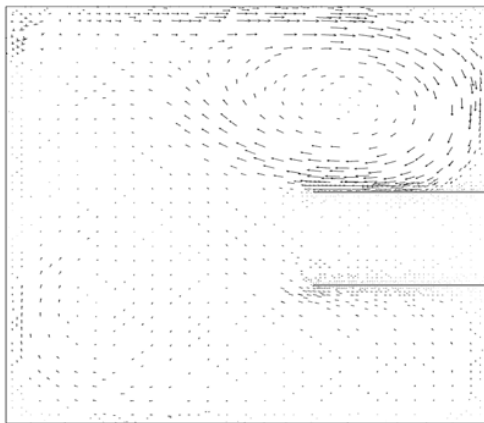
the second layer, and the flow strength is large, especially in the area close to the bracket.



(a) $X = 0$ m cross section



(b) $X = 0.25$ m cross section



(c) $X = 0.45$ m cross section

Fig. 6 $V = 0.8$ m/s, $X = 0$ m \ $X = 0.25$ m \ $X = 0.45$ m cross section velocity vector

B. Structure of Bottom-Entering and Bottom-Out

The gas inside the tank flows into the box from the bottom inlet and flows out of the box from the bottom outlet. The remaining conditions are the same with the last section, and the model is shown in Fig. 7.

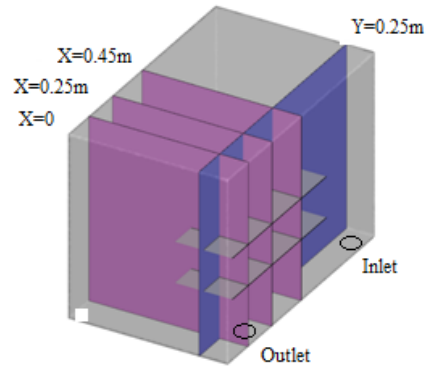


Fig. 7 Calculation model of bottom-entering and bottom-out structure

Fig. 8 shows the velocity vector of $Y = 0.25$ m cross section at 0.8 m/s wind speed. Fig. 9 shows the $Y = 0.25$ m cross section velocity plot at $V = 0.8$ m/s.

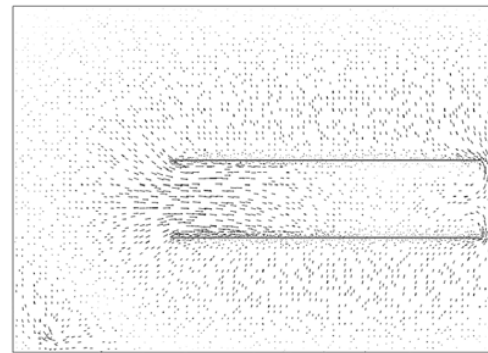


Fig. 8 $V = 0.8$ m/s, $Y = 0.25$ m cross section velocity vector of bottom entering and out structure

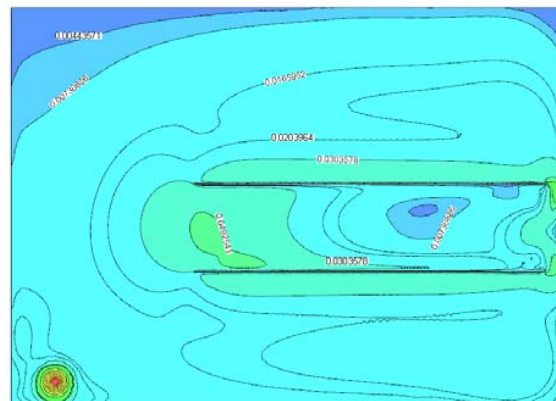


Fig. 9 $V = 0.8$ m / s, $Y = 0.25$ m cross section velocity sketch of bottom entering and out structure

Fig. 10 shows the 0.8 m/s wind speed, $X = 0$ m, 0.25 m and 0.45 m cross section of the velocity vector.

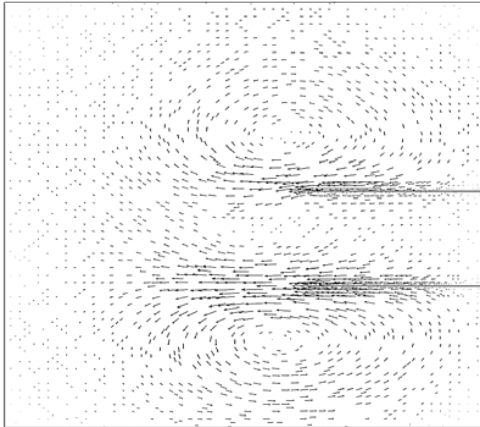
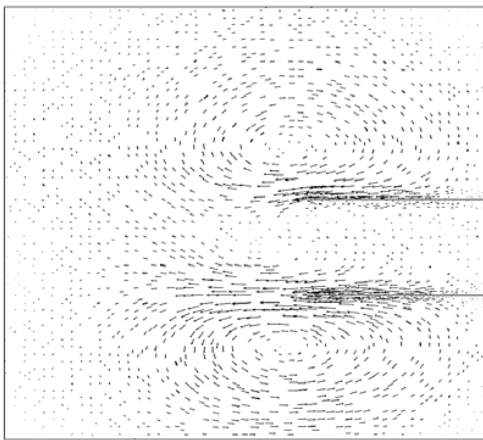
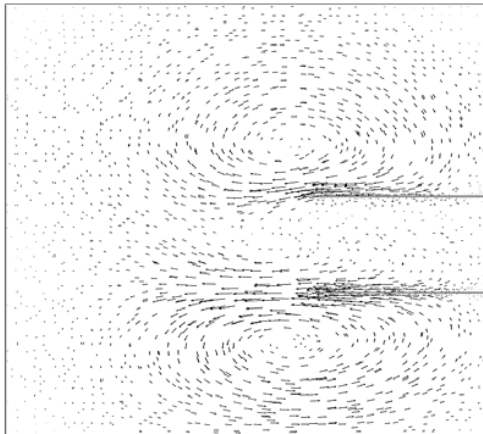
(a) $X = 0$ m cross section(b) $X = 0.25$ m cross section(c) $X = 0.45$ m cross section

Fig. 10 $V = 0.8$ m/s, $X = 0$ m \ $X = 0.25$ m \ $X = 0.45$ m cross section velocity vector of bottom entering and out structure

IV. CONCLUSION

In this paper, the influence of different inlet position and gas flow on the internal flow field disturbance is calculated. The

calculation results show that: The top-entering and bottom-out structure, airflow disturbance on the left side of the box is serious, that is not convenient for the operation of the sample.

The bottom entering and out structure effectively reduce the disturbance of the airflow in the main operating area on the left side of the box, and there is a relatively strong disturbance in the bay part. The sample encapsulated in the sample box has little effect on the disturbance of the airflow.

REFERENCES

- [1] J. H. Allton and T. J. Beville, "Curatorial Statistics on Apollo Regolith Fragments Applicable to Sample Collection by Raking," *Adv Space Res.*, vol. 31, no. 11, pp. 2305-2313, 2003.
- [2] W. Q. Tao, *Numerical Heat Transfer*. Xi An: Xi An Jiaotong University Press, 1998.
- [3] P. Zeng, *Finite Element Foundation Tutorial*. Beijing: Higher Education Press, 2009.
- [4] Y. H. Chen, Q. Wang and M. B. Piao, "Development of Turbulence Model and Its Research Status," *Energy and Environment*, no. 2, pp. 4-7, 2009.
- [5] Z. Q. Zhu, *Applied Computational Fluid Mechanics*. Beijing: Beijing University of Aeronautics and Astronautics Press, 2009.